International Journal of Nanomedicine

Dovepress
open access to scientific and medical research

Open Access Full Text Article

ORIGINAL RESEARCH

Delivery vehicle of muscle-derived irisin based on silk/calcium silicate/sodium alginate composite scaffold for bone regeneration

This article was published in the following Dove Medical Press journal:
International Journal of Nanomedicine

Xianzhen Xin[1,*]
Jiannan Wu[1,*]
Ao Zheng[1]
Delong Jiao[1]
Yang Liu[2]
Lingyan Cao[1]
Xinquan Jiang[1]

[1]Department of Prosthodontics, Shanghai Engineering Research Center of Advanced Dental Technology and Materials, Shanghai Key Laboratory of Stomatology and Shanghai Research Institute of Stomatology, National Clinical Research Center for Oral Diseases, Shanghai Ninth People's Hospital, College of Stomatology, Shanghai Jiao Tong University School of Medicine, Shanghai, China; [2]The State Key Laboratory of Bioreactor Engineering, East China University of Science and Technology, Shanghai, China

*These authors contributed equally to this work

Background: Irisin is a cytokine produced by skeletal muscle and usually plays a pivotal role in inducing fat browning and regulating energy expenditure. In recent years, it was found that irisin might be the molecular entity responsible for muscle–bone connectivity and is useful in osteogenesis induction.

Materials and methods: To study its effect on bone regeneration, we developed silk/calcium silicate/sodium alginate (SCS) composite scaffold based on an interpenetrating network hydrogel containing silk fibroin, calcium silicate, sodium alginate. Then we loaded irisin on the SCS before coating it with polyvinyl alcohol (PVA). The SCS/P scaffold was physically characterized and some in vitro and in vivo experiments were carried out to evaluate the scaffold effect on bone regeneration.

Results: The SCS/P scaffold was showed a porous sponge structure pursuant to scanning electron microscopy analysis. The release kinetics assay demonstrated that irisin was stably released from the irisin-loaded hybrid system (i/SCS/P system) to 50% within 7 days. Moreover, osteoinductive studies using bone marrow stem cells (BMSCs) in vitro exhibited the i/SCS/P system improved the activity of alkaline phosphatase (ALP) and enhanced the expression levels of a series of osteogenic markers containing Runx-2, ALP, BMP2, Osterix, OCN, and OPN. Alizarin red staining also demonstrated the promotion of osteogenesis induced by i/SCS/P scaffolds. In addition, in vivo studies showed that increased bone regeneration with better mineralization and higher quality was found during the repair of rat calvarial defects through utilizing the i/SCS/P system.

Conclusion: These data provided strong evidence that the composite i/SCS/P would be a promising substitute for bone tissue engineering.

Keywords: silk fibroin, biocompatible scaffold, bone regeneration, irisin, delivery vehicle

Correspondence: Xinquan Jiang; Lingyan Cao
Department of Prosthodontics, Shanghai Engineering Research Center of Advanced Dental Technology and Materials, Shanghai Key Laboratory of Stomatology and Shanghai Research Institute of Stomatology, National Clinical Research Center for Oral Diseases, Shanghai Ninth People's Hospital, College of Stomatology, Shanghai Jiao Tong University School of Medicine, 639 Zhizaoju Road, Shanghai 200011, China
Tel +86 21 2327 1699; +86 21 5331 5741
Email xinquanj@aliyun.com; linya.lingyancao@gmail.com

Introduction

Bone tissue is a complex organ that contains a collagenous fibrous matrix and nanocrystals of carbonated apatite. Bones play an important role in organisms. In addition to providing machinal support and protection, bones also participate in ion homeostasis and hematopoiesis.[1–4] Conditions such as trauma, tumors, and inflammation will impair the structure and functions of bone, thus resulting in bone defects that, in turn, significantly impact psychological health and the quality of life.[5] To overcome the limitations of traditional bone grafting, tissue engineering has become the strategy with the most potential for the clinical treatment of bone defects.[6] Tissue engineering approaches are mainly based on the use of scaffolding biomaterials, seed cells and growth factors/molecules.[7]

submit your manuscript | www.dovepress.com
Dovepress
http://dx.doi.org/10.2147/IJN.S193544

Bone regeneration involves many bioactive factors with different effectiveness characteristics among the miscellaneous growth factors involved in bone tissue engineering.[8–11] The bioactive molecules involved in muscle–bone connection should be stressed due to the close relationship between skeletal muscle and bone.[12] Physical exercise, which is utilized as a nonpharmacological intervention in treatment protocols for some diseases, has been considered as being advantageous to metabolic and bone health.[13,14] Numerous studies have been designed to detect the molecules involved in the link between physical activity and bone acquisition and maintenance.[15] In recent years, attention has focused on irisin, which is a cytokine produced by skeletal muscle that exerts a hormone-like effect.[16] It has been demonstrated that irisin plays pivotal roles in inducing fat browning and regulating energy expenditure.[17–19] It is reported that myokine irisin is potentially the molecular entity responsible for muscle–bone connectivity.[20] Many studies have reported that irisin could be found in the circulation and generated by skeletal muscle during physical activity.[21] Irisin has also been investigated as a point of connection between bone metabolism and physical activity[22] due to its ability to induce the differentiation of BMSCs into mature osteoblasts.[12] Hence, irisin might be selected as an effective factor to induce bone regeneration.

To load and protect irisin against degradation for in vivo applications, a delivery system is necessary since it could provide a local retention and activity protection of irisin.[23–25] Previously, we prepared silk/calcium silicate/sodium alginate (SCS) composite scaffolds, which showed compatibility with bone marrow stem cells (BMSCs) and good biological properties.[26] The porous structure could provide growth spaces for cells, and release of ions such as Ca and Si from the scaffold might promote the osteogenesis of BMSCs. These advantages of SCS scaffolds indicate that it may be used as a vector as a marginally aggressive biomaterial for osteogenesis in vivo. However, for the controlled release of general proteins, especially for that of irisin (12–36 kDa, several nanometers of dimer size measured by PyMOL, version 2.2.3, Schrodinger LLC, New York, NY USA),[27] the pore size of the SCS scaffold, which is approximately hundreds of micrometers, seems rather large. Therefore, modification of the SCS scaffold was necessary for better control of the release of irisin. Polyvinyl alcohol (PVA) is a hydrophilic polymer with a large number of hydroxyl groups in its molecular structure. It is especially suitable for the application in the biomedical field because of its nontoxicity, nonimmunogenicity, noncarcinogenicity, good biocompatibility, and inertness in body fluids.[28] At present, PVA has been widely used as the surface-coating material for controlled drug release.[29–31] Therefore, PVA could be chosen in this study to coat the SCS scaffold. It is suspected that after loaded with irisin, SCS scaffold would be treated with a very quick soak in PVA aqueous solution and then dried at room temperature to form a PVA membrane outside the scaffold. The pores on the scaffold surface were assumed to be covered by the PVA membrane and the rapid diffusion release of the absorbed irisin in these pores, which mainly contribute to the burst release of irisin, might be remarkably decreased until the dissolution of PVA.

The objective of the present study was to detect the potential of irisin usage as a bioactive factor for bone tissue regeneration in vivo using the SCS scaffold as a delivery vehicle. We aimed to develop a composite scaffold based on a hydrogel with a stable dual network structure. We introduced calcium silicate (CS) into the blend of silk fibroin (SF) solution and sodium alginate (SA) solution. With the addition of vitamin C (VC), uniformly distributed CS particles were induced to release Ca^{2+} in the mixture gradually. Meanwhile, SF could gel through a Ca^{2+}-triggered β-sheet conformation, and SA could be crosslinked by Ca^{2+}. Thus, the blend could in situ form an interpenetrating network hydrogel. After lyophilization, we obtained the scaffold and used it for irisin delivery. For a prolonged release of irisin, a coating layer made from PVA was developed on the surface of the irisin-loaded scaffold. In this study, a series of tests was performed to assess the effects of the irisin-loaded composite scaffold (i/SCS/P) on osteogenesis and bone regeneration in vivo. We hypothesized that the i/SCS/P scaffold would not only deliver irisin but also help promote its osteogenic ability by releasing pro-osteogenic ions (Figure 1). The synergy between irisin and the SCS/P scaffold might be a promising strategy for use in bone regeneration.

Materials and methods

Fabrication of SCS, SCS/P, and i/SCS/P composite scaffolds

The SF/CS/SA (SCS) scaffolds were prepared according to our previous method.[26] In short, SF was first extracted from domesticated silkworm cocoons.[26] Then, we prepared 6% (w/v) SF, 2% (w/v) SA (Sigma-Aldrich Co., St Louis, MO, USA) and 10% (w/v) VC aqueous solutions for subsequent use. Next, 10.5 mg of CS particles was added to a 1 mL mixed solution of silk fibroin and sodium alginate (SF/SA, V/V=7/3) and dispersed uniformly. Then, 100 μL of the VC aqueous solution was slowly dropped into the SF/CS/SA mixed solution under stirring, and the mixture was then poured into a cylindrical polytetrafluoroethylene mold and allowed to gel at 37°C. The resulting composite hydrogel was then subjected to freeze-drying. To prepare the biocompatible scaffold loaded

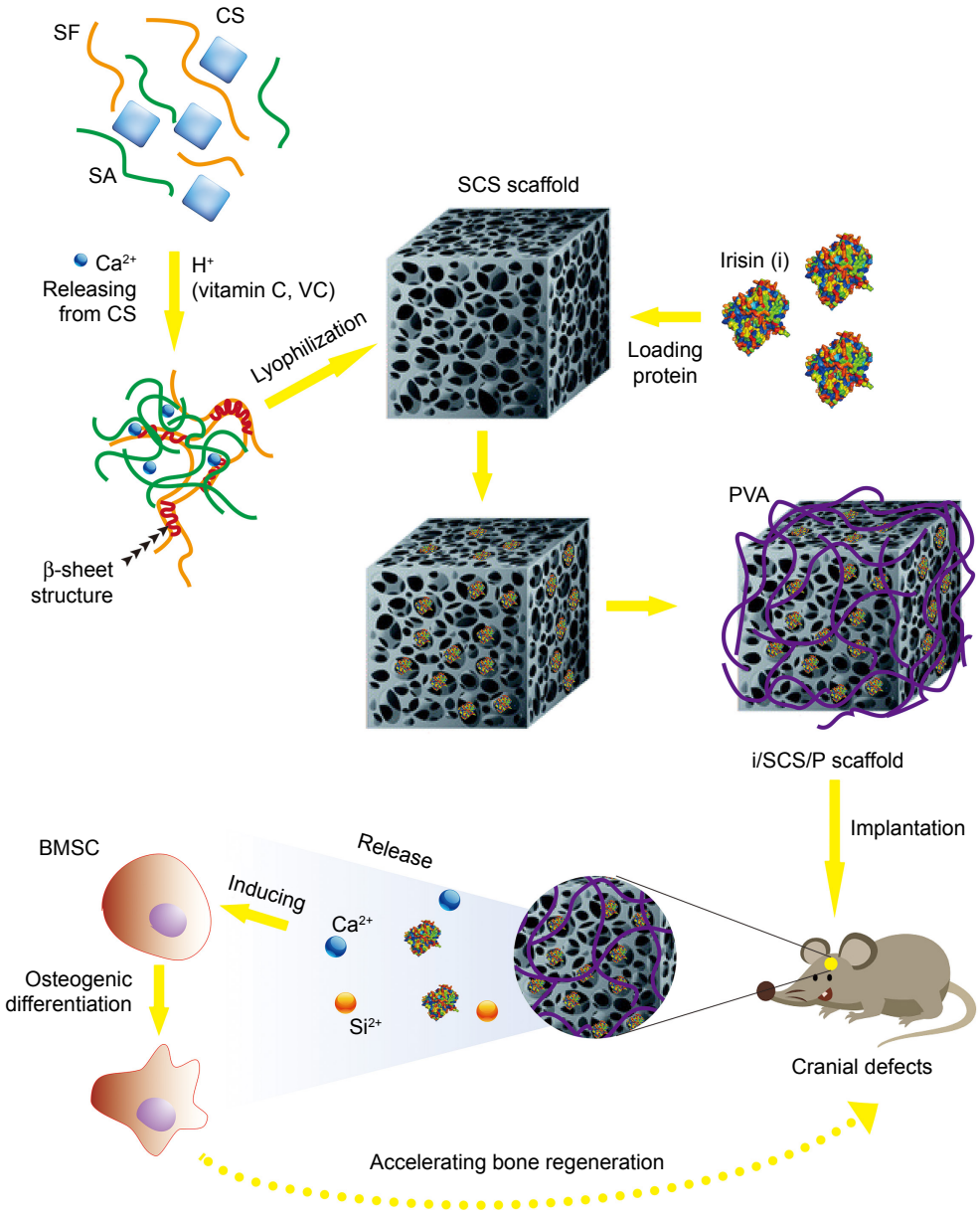

Figure 1 Schematic diagram of preparation of irisin loaded SCS/P scaffold and its application for bone regeneration.
Abbreviations: SF, silk fibroin; CS, calcium silicate; SA, sodium alginate; SCS, silk/calcium silicate/sodium alginate; BMSCs, bone marrow stem cells; i/SCS/P, irisin-loaded silk/calcium silicate/sodium alginate/PVA composite scaffold; SCS/P, silk/calcium silicate/sodium alginate/PVA.

with irisin, an irisin aqueous solution containing a certain amount of irisin was uniformly dropped onto the SCS scaffold (10 mm diameter, 3 mm height) and then lyophilized. The lyophilized irisin-loaded SCS scaffold was placed in a 10% PVA aqueous solution for 10 minutes and then dried at room temperature to form a PVA coating layer. We named this irisin-loaded scaffold i/SCS/P. For the composite scaffold without irisin, we named it SCS/P.

Scaffold characterization

The surfaces of the SCS and SCS/P scaffolds were observed by scanning electron microscopy (SEM, SU8220, Hitachi Ltd., Tokyo, Japan). At least five fields were acquired and imaged for each substrate, and the pore size was measured by a blinded observer using the ImageJ 1.45 software (NIH, Bethesda, MD, USA). The elemental composition of the scaffold surface and its distribution was further determined by energy dispersive spectroscopy (EDS, Ultim Max, Oxford Instruments, Abingdon, Oxfordshire, UK). The swelling and degradation properties of the SCS and SCS/P scaffolds were investigated as described below. The sample was weighed (W1) immediately after freeze-drying and then immersed in PBS at 37°C. At each determined time point, the sample was taken out, washed, and the excess

buffer on the scaffold was blotted with filter paper. The weight of the wet sample (W2) and that of the freeze-dried sample (W2′) was recorded. The swelling and degradation ratio were respectively calculated according to the formulas Swelling%=[(W2−W1)/W1]×100% and degradation ratio %=(W1−W2′)/W1 ×100%. In order to confirm the degradation of the prepared scaffolds in protease XIV solution, we carried out the investigations according to the reported procedures.[32] The sample was weighed (W3) immediately after freeze-drying and then immersed in deionized water for 24 hours to leach out soluble peptides. After that, the sample was immersed in 5 mL of protease XIV solution (0.23 μg/mL) at 37°C. Protease XIV from *Streptomyces griseus* (specific activity: ≥3.5 U/mg protein) was purchased from Sigma-Aldrich Co. At 1, 2, 3, 4 and 5 day, the sample was taken out and washed with deionized water for 48 hours, respectively. After washing, the sample was freeze-dried and weighed (W4). Degradation ratio %=(W3−W4)/W3 ×100%. Each test was carried out in triplicate, and the results were expressed as the mean ± SD values. The compression performance of the SCS and SCS/P scaffold (10 mm diameter, 3 mm height) was measured using an electronic universal testing machine (HY-0230, Hengyi Testing Instruments, Shanghai, China) at room temperature under a constant strain rate of 2 mm/min. The elastic modulus of the scaffold was determined by plotting the stress–strain curve and calculating the slope of the curve within 50% of the deformation, while the corresponding stress was considered to be the compressive strength within 50% deformation. Six replicates per group were tested, and the results were expressed as the mean ± SD. In addition, the sample was immersed in PBS, and the pH of the environmental solution at different time points within 24 hours was measured using a pHS-2C system (Jinke Leici Company, Shanghai, China) to evaluate the acidity and alkalinity of the SCS/P scaffold.

Bioactivity of the SCS/P scaffolds

Each sample of SCS/P scaffold was immersed in 30 mL of simulated body fluid (SBF) at 37°C. The SBF solution was preconfigured according to the reported protocol.[33] After soaking for 7 days, the sample was taken out for washing and then lyophilized. The surface morphology of the immersed scaffold was observed by SEM (S-3400, Hitachi Ltd.). The crystal structure of the scaffold surface before and after soaking was analyzed by X-ray diffractometry (XRD, PANalytical B.V, Almelo, the Netherlands) at room temperature. Cu Kα radiation, a scanning speed of 2°/min and a 2θ angle range of 10° to 70° were selected as the detection parameters.

Release kinetics of irisin from the i/SCS/P scaffold

The i/SCS/P scaffold (10 mm diameter, 3 mm height) loaded with 2 μg irisin was placed in 5 mL of PBS (pH 7.4) and stirred at 15 rpm. At each predetermined time point, 1 mL of the supernatant containing the released irisin was separately collected after centrifugation (10,000 × g, 37°C, 10 minutes) and replaced with an equal volume of fresh PBS buffer. The concentration of irisin in the supernatant was determined using a Human Irisin ELISA Kit (Sigma-Aldrich Co.) according to the manufacturer's instructions, and then the cumulative release of irisin at each time point was calculated. Each test was carried out in triplicate, and the results were expressed as the mean ± SD values.

In vitro biological investigations

Extraction and culture of bone marrow stem cells (BMSCs)

Rat BMSCs were isolated from 4-week-old Sprague Dawley rats (Shanghai SLAC Experimental Animal Center, Shanghai, China). According to previous studies,[34] the femur was isolated and cut at the epiphysis after the rat was intraperitoneally injected with pentobarbital for euthanasia. Bone marrow was flushed quickly using DMEM supplemented with 10% FBS (Thermo Fisher Scientific, Waltham, MA, USA), 100 U/mL penicillin, and 100 μg/mL streptomycin and collected by centrifugation. The harvested cells were incubated in the abovementioned DMEM at 37°C in humidified air/5% CO_2. The culture medium was changed every 3 days. All animals were from the Animal Center of Shanghai Ninth People's Hospital. All experimental protocols regarding the use of animals in this study were approved by the Institutional Animal Care and Use Committee and followed the procedure for Animal Experimental Ethical Inspection of the Ninth People's Hospital, which is affiliated with Shanghai Jiao Tong University School of Medicine.

Biocompatibility of the SCS and SCS/P scaffolds

BMSCs were seeded into 24-well culture plates at a seeding density of $5*10^4$/well. After 12 hours, the SCS and SCS/P scaffolds were placed in a transwell chamber and indirect cultured with BMSCs, respectively. According to the manufacturer's protocol, after 1, 3, and 7 days of culture, the medium was exchanged with fresh medium containing CCK-8 reagent (Dojindo, Kumamoto, Japan), followed by incubation at 37°C for another 1.5 hour. Then, the absorbance of the solution at 490 nm was measured using a microplate reader (Spark 10M, Tecan, Switzerland). Cells seeded into

DMEM containing 10% FBS inoculated onto a well plate without indirect culture with the scaffolds were used as a control group.

Effect of irisin on cell proliferation

BMSCs were seeded into 96-well culture plates at a seeding density of $5*10^3$/well. After 12 hours, the culture medium containing different concentrations of irisin (50, 100, 200 μg/L) was replaced. According to the manufacturer's protocol, after 1, 3, and 7 days of culture, CCK-8 reagent (Dojindo) was used for another 1.5 hours of incubation at 37°C to detect cell proliferation. The absorbance of the solution at 490 nm was measured using a microplate reader (Spark 10M). Cells seeded onto a culture plate supplemented with DMEM containing 10% FBS were used as a control group.

Bioactivity of the released irisin

For the bioactivity assessment of the released irisin, an i/SCS/P scaffold (10 mm diameter, 3 mm height) loaded with 2 μg irisin was incubated in 5 mL culture medium (DMEM containing 10% FBS) at 37°C for, respectively, 4 hours, 12 hours, and 7 days. Under sterile conditions, the supernatants were respectively gathered by centrifugation at each scheduled time. The irisin concentration in the supernatant was determined using a Human Irisin ELISA Kit (Sigma-Aldrich Co.). Then, the biological activity of the released irisin was evaluated by measuring the ability of the extract of i/SCS/P scaffold to induce alkaline phosphatase (ALP) activity in BMSCs. BMSCs were seeded at density of $5*10^4$ cells/well into 24-well culture plates and allowed to fully adhere. The supernatants containing the released irisin collected at 4 hours, 12 hours, and 7 days were then used to culture BMSCs. Culture medium containing equal amounts of irisin was also prepared as a control to culture BMSCs. An ALP activity assay was performed 3 days later, and the results were normalized to the total protein content. To visualize the ability of irisin released from the i/SCS/P scaffolds to induce ALP activity in BMSCs, we seeded BMSCs into 48-well plates at a density of $3*10^4$ cells/well. The extract of the i/SCS/P scaffold obtained above was used for BMSCs culture. BMSCs cultured with the extracts of SCS/P scaffolds were used as a control. After 7 days, a BCIP/NBT alkaline phosphatase color development kit (Beyotime, Shanghai, China) was used for ALP staining according to the instruction manual. After 28 days of culture, alizarin red S (ARS) staining (Beyotime, Shanghai, China) was utilized to evaluate the matrix mineralization. Both ALP staining and the mineralized matrix were observed through an inverted optical microscope (Nikon Corporation, Tokyo, Japan).

Quantitative real-time PCR (qRT-PCR) assay

BMSCs were seeded into 48-well plates at a density of $3*10^4$ cells/well. After adhesion, the extract of the i/SCS/P scaffold was replaced into each well for BMSCs culture, while the extract of the SCS/P scaffold was used as a control. The total RNA was isolated from BMSCs using TRIzol™ reagent (Thermo Fisher Scientific) after 3 and 7 days of culture, respectively. The RNA concentration was determined using a NanoDrop spectrophotometer (ND-1000; Thermo Fisher Scientific), and cDNA synthesis was carried out using a reverse transcription kit (Takara, Tokyo, Japan). qRT-PCR analysis of osteogenic markers such as RUNX2, ALP, Osterix, BMP2, OCN, and OPN was performed using a ROCHE480 real-time PCR system (LightCycler480, Hoffman-La Roche Ltd., Basel, Switzerland). Normalization was performed using *GAPDH* as an internalization gene. The gene expression of the control group was taken as 1, and those of the other groups were expressed as changes in terms of relative fold for data analysis. The primer sequences used in this experiment were commercially synthesized, and the specific primer sets are listed in Table 1. All experiments were carried out in triplicate.

Repair of calvarial defect in vivo

Surgical procedures

Twelve male Sprague Dawley rats of 4 weeks old were used. As described previously,[35] a circular defect of 5 mm in diameter was surgically excised on both sides of the skull after anesthesia. All rats were randomly divided into four groups (three in each group, with each group containing six defects) for implantation of the four different kinds of scaffolds into the skull defects (blank: no implantation; 0: implantation of SCS/P scaffold; 100: implantation of i/SCS/P scaffold containing 100 ng irisin; and 200: implantation of i/SCS/P scaffold containing 200 ng irisin). The incision was then sterilized and sutured. Animals were then subcutaneously injected with antibiotics (streptomycin and penicillin) to prevent infection. At 8 weeks postoperation, the animals were sacrificed, and tissue blocks including the original defect sites were cut out and fixed in 4% paraformaldehyde for subsequent study.

Microcomputed tomography (μCT) analysis

The fixed tissue samples were scanned using a high-resolution μCT (μCT-80, Scanco Medical AG, Zurich, Switzerland) to observe and evaluate the morphology and quality of

Table 1 Quantitative real-time PCR primer sets

Gene	Direction	Sequence (5′–3′)
RUX-2	Forward	GCGGACGAGGCAAGAGTT
	Reverse	TTGGTGCTGAGTTCAGGGAG
ALP	Forward	TCACTTCCGCCCGGAACCCT
	Reverse	TGTCCTGCCGGCCCAAGAGA
Osterix	Forward	GCAAGCTTTCGCCACCATGGCGTCCTCTCTGCTTGAGGA
	Reverse	ATGAATTCTTCTATTATCAGATCTCTAGCAGGTTGC
BMP2	Forward	TGGGTTTGTGGTGGAAGTGGC
	Reverse	TGGATGTCCTTTACCGTCGTG
OCN	Forward	GCCCTGACTGCATTCTGCCTCT
	Reverse	TCACCACCTTACTGCCCTCCTG
OPN	Forward	CCAAGCGTGGAAACACACAGCC
	Reverse	GGCTTTGGAACTCGCCTGACTG
GAPDH	Forward	GGC AAG TTC AAC GGC ACA G
	Reverse	CGC CAG TAG ACT CCA CGA CAT

the newly formed bone in the skull defect (pixel matrix, 1,024×1,024; slice increment 10 μm). Using Scanco software (Scanco Medical AG), the region including the original defect site and the surrounding tissue was circled carefully, and the upper threshold of 225 and the lower threshold value of 90 were selected to perform three-dimensional reconstruction of the sample. The new bone volume (BV) and new bone mineral density (BMD) inside the original defect site were quantitatively analyzed by μCT as previously described.[36] In total, six parallel samples per group were analyzed, and the results were expressed as the mean ± SD values.

Histology analysis

The fixed tissue samples were decalcified in 10% EDTA for 30 days and then embedded in paraffin. The embedded sample was then cut into 4 μm-thick sections. H&E staining was performed, and the samples were observed through an inverted optical microscope (Nikon Corporation). Three parallel samples per group were treated for histology analysis.

Statistical analysis

Quantitative analysis in this study was accomplished using Prism 7 (GraphPad Software, Inc., La Jolla, CA, USA). All quantitative results were expressed as the mean ± SD. Statistical comparisons between the designated groups were calculated using ANOVA with a statistical significance confidence level >95% ($P<0.05$).

Results and discussion

Physical characterization

The morphology of the optimized SCS scaffold was imaged using SEM (Figure 2A). The SCS scaffolds showed a porous structure composed of interconnected pores with a uniform size of 300±12 μm. An uneven surface with obvious particles buried in the pore walls of the SCS scaffold (Figure 2B) could be found. Compared with the SCS scaffolds, the SCS/P scaffold showed a rough surface with unopen pores (Figure 2C). The PVA coating on the SCS/P scaffold covered the particles on the pore wall and formed a folded orifice surface (Figure 2D). According to the section morphology study of the SCS/P scaffold, the coated PVA did not affect the inner structure of the porous scaffolds (Figure S1), and the interconnected pores were beneficial to cells accessing the inside of the scaffold and to commutation of the body fluid.[37] Owing to the water solubility of PVA, it could dissolve slowly in the surrounding liquid and then the pores on the scaffold surface showed again. Meanwhile, the adhered cells would enter into the scaffold. We further evaluated the elemental distribution and composition of the surfaces of the SCS and SCS/P scaffolds by EDS, respectively. EDS mapping of the elemental distribution (Figure 2E) suggested that the aggregation of Si and Ca elements on the SCS scaffold surface appeared at the site where the embedded particles existed. This result confirmed that the particles buried in the pore walls of the SCS scaffold were CS granules. After PVA coating, the distribution of Si and Ca elements on the SCS/P scaffold surface seemed more uniform, without remarkable aggregation. Additionally, upon comparing the SCS scaffold with the SCS/P scaffold, quantitative analysis of all the elements on the selected scaffold surface (Figure 2F and G) showed a significant decrease of the peak intensity of the Si and Ca elements, which indicated that the surface of the SCS/P scaffold was covered by a layer of PVA.

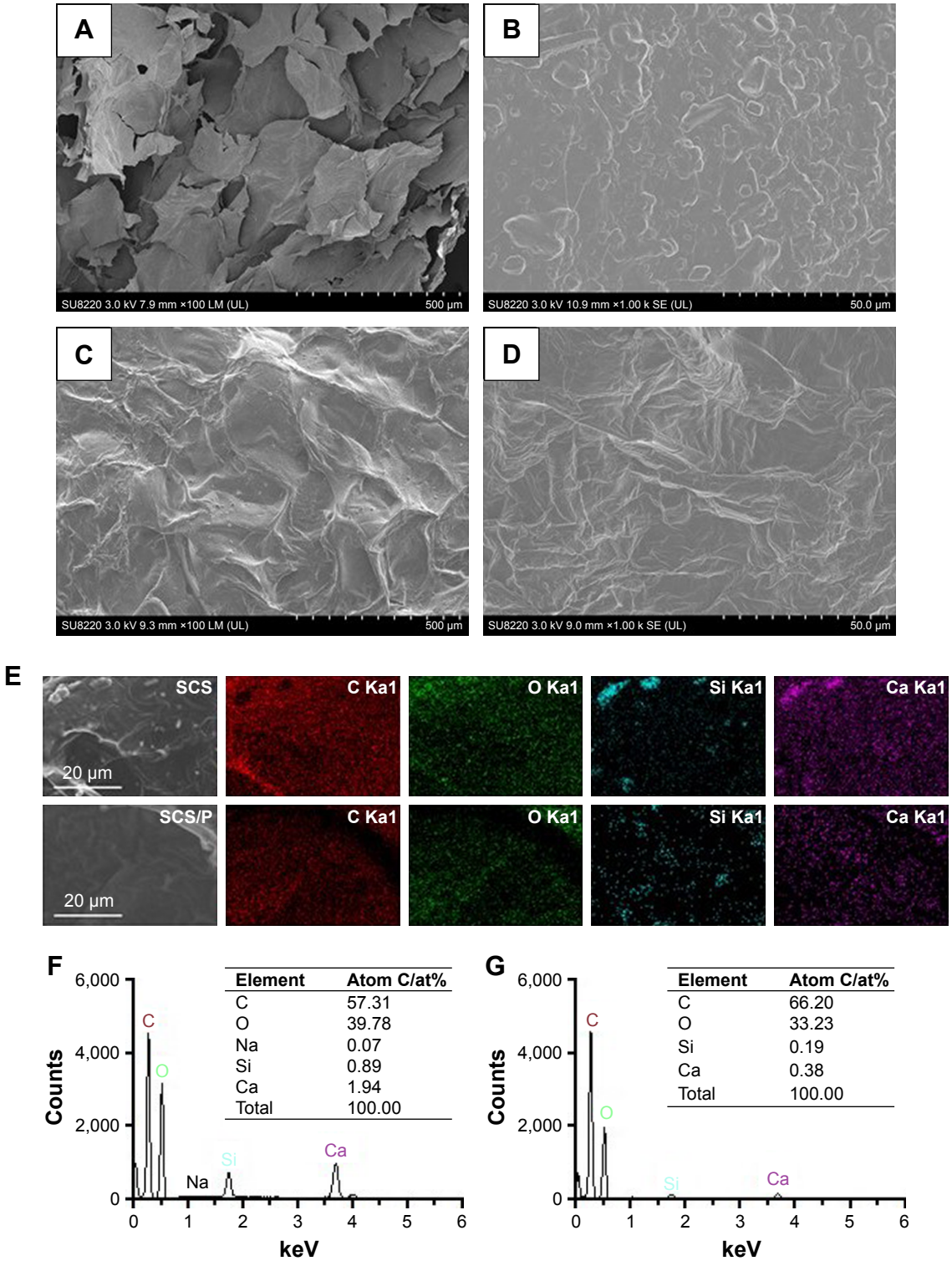

Figure 2 Morphology and composition analysis.
Notes: SEM images of SCS (**A** and **B**) and SCS/P (**C** and **D**) scaffold. (**E**) Selected area on SCS and SCS/P scaffolds and the elemental distributions of C, O, Si, Ca. (**F**) Quantitative analysis of all the elements on the SCS scaffold surface. (**G**) Quantitative analysis of all the elements on the SCS/P scaffold surface.
Abbreviations: SEM, scanning electron microscopy; SCS, silk/calcium silicate/sodium alginate; SCS/P, silk/calcium silicate/sodium alginate/PVA.

After a series of physical characterizations including determination of the swelling and degradation ratio, pH, and mechanical properties, the properties of the SCS/P scaffolds were obtained (Figure 3). The SCS/P scaffold was prepared from a hydrogel, so we investigated its swelling and degradation ratio (Figure 3A and B). The results showed that when immersed in PBS, the SCS/P scaffold could rapidly adsorb the solution and increase its weight

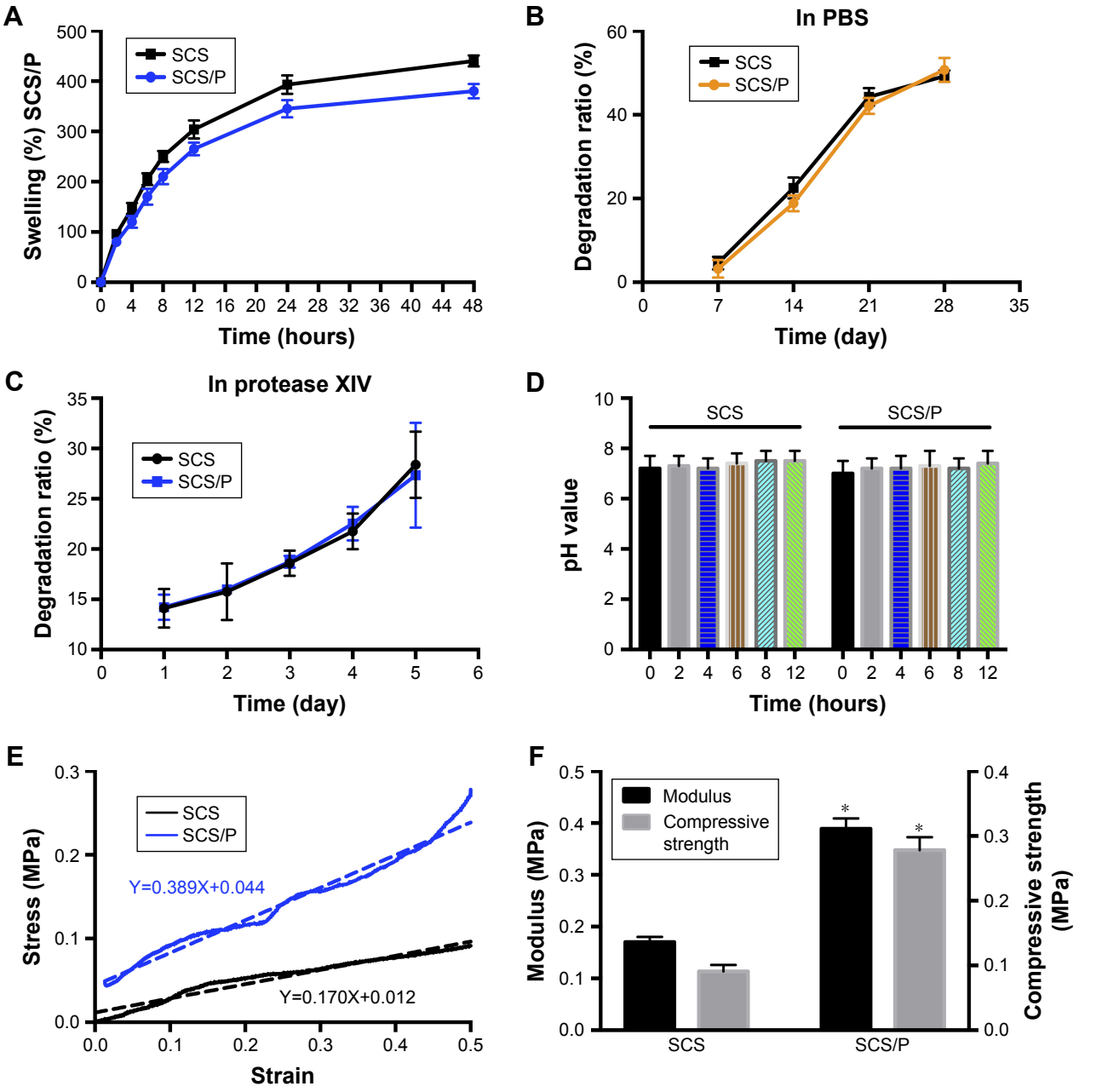

Figure 3 Physical characterizations of SCS/P composite scaffold.
Notes: (**A**) Swelling ratio. (**B**) Degradation curve in PBS. (**C**) Degradation curve in protease XIV solution. (**D**) pH value changes. (**E**) Compressive stress-strain curve. The dotted line stands for fitted line of function. (**F**) Compressive modulus and strength. *$P<0.05$, compared with SCS group.
Abbreviations: SCS, silk/calcium silicate/sodium alginate; SCS/P, silk/calcium silicate/sodium alginate/PVA.

to the swelling ratio of 265%±13% by 12 hours, followed by relatively slow swelling to 380%±15% within 48 hours. In comparison, swelling ratio of SCS scaffold was slightly larger than SCS/P scaffold. According to the swelling test, we found that after rehydration, both the SCS and SCS/P scaffolds adsorbed PBS solution and became composite hydrogels again, which means that the pores in the lyophilized scaffolds disappeared after immersion in PBS and were replaced by water. Actually, we believed that in hydrated state, the structure differences between the SCS and SCS/P would not be so high. Figure 3B demonstrates that the degradation of the SCS/P scaffold in PBS increased with time from 3.2% at 7 days to 50.7% at 28 days. When immersed in protease XIV solution (Figure 3C), the degradation of the SCS/P scaffold increased with time from 14.12% at 1 day to 27.34% at 5 days, which was similar to the degradation rate of SCS scaffold. Generally speaking, the PVA coating was not influential to the degradation of the SCS and SCS/P scaffold; this is possibly because of the water solubility of PVA. As the degradation rate was vital to cell adhesion and differentiation, the degradation rate of SCS/P is of possible benefit to bone differentiation.[38]

As shown in Figure 3D, the SCS/P scaffold showed stable pH values at ~7.2 after soaking in PBS for 12 hours. In tissue engineering, the pH of the culture environment required by seed cells is generally 7.2–7.4. Stem cell behaviors sensitively respond to pH changes. It has been reported that BMSCs had lower osteogenic gene expressions at low pH, while the ALP activity and gene expression was relatively lower.[39] Thus, the acidity and alkalinity of the scaffolds also play an important role in regulating the proliferation and differentiation of stem cells. Figure 3E and F showed the mechanical properties of the SCS/P scaffold. There is a linear relationship between the stress and strain of the SCS/P within 50% deformation, as determined by a constant-rate compression test. The elastic modulus of the SCS/P was 0.39±0.02 MPa and the compressive strength was 0.28±0.02 MPa with 50% deformation which was significantly increased compared to those of the SCS scaffold. As reported,[40] the mechanical properties of the porous scaffolds were closely related to their porosity. By reducing the porosity, the mechanical strength of the scaffold was significantly increased. According to our previous research,[26] the incorporation of CS into the SCS scaffold could significantly reduce the scaffold porosity and make its porous structure dense, providing the silk scaffold with better mechanical properties. Studies have shown that the mechanical properties of materials also have an important impact on stem cell differentiation.[41] It is beneficial for the osteogenic differentiation of BMSCs cultured on a biomaterial when the surface modulus is raised.[42]

Bioactivity of SCS/P scaffolds

From Figure 4A and B, we found that a layer clearly formed on the surface of the SCS/P scaffold when the porous material was soaked in SBF for 7 days, and rough structures could

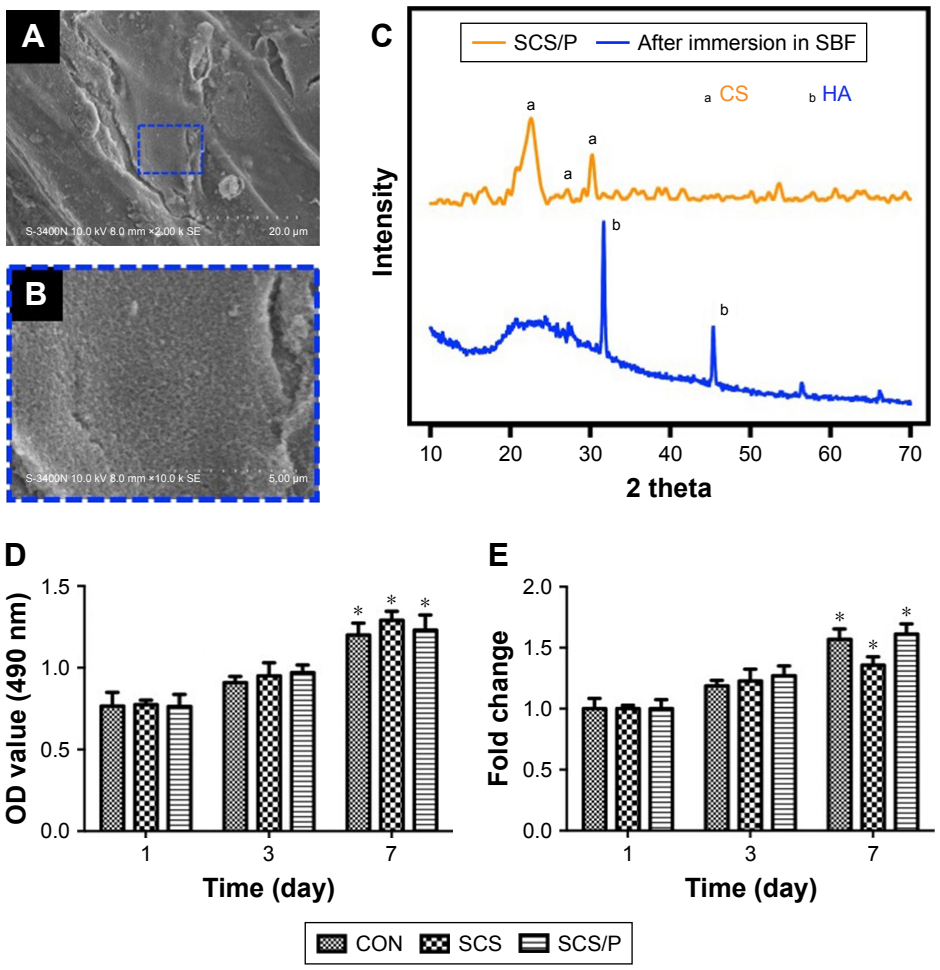

Figure 4 Bioactivity and biocompatibility of SCS/P composite scaffold.
Notes: (**A**) SEM image of SCS/P scaffold after immersed in SBF after 7 days. The region of interest is selected by a blue dashed outline and magnified in (**B**). (**C**) XRD spectra of SCS/P scaffold immersed in SBF after 7 days (blue line) and untreated by SBF (yellow line). (**D**) Cell viability and (**E**) the fold change of BMSCs co-cultured with SCS and SCS/P composite scaffolds. Cells cultured without SCS or SCS/P composite scaffolds were used as control (CON). *$P<0.05$, compared with the corresponding data at day 1.
Abbreviations: SCS/P, silk/calcium silicate/sodium alginate/PVA; SBF, simulated body fluid; CS, calcium silicate; HA, hydroxyapatite; CON, control; SCS, silk/calcium silicate/sodium alginate; SEM, scanning electron microscopy; BMSCs, bone marrow stem cells.

also be detected on the dense deposit layer. In Figure 4C, [a] indicated peaks belonging to CS while [b] indicated peaks belonging to HA. Compared to the XRD data of SCS/P scaffold before and after soaking in SBF for 7 days, we found that the intensity of peaks (2θ=22.8°, 27.5°, 30.4°) belonging to CS was decreased; meanwhile, the intensity of peaks (2θ=32.3°, 45.4°) belonging to HA was increased. This result indicates that HA crystal formed on the surface of SCS/P scaffolds. This result corroborated that the SCS/P scaffold still showed a good biological activity after coating with PVA. The similar bioactivity of SCS scaffold was confirmed in our previous study.[26]

Release kinetics of irisin from the i/SCS/P scaffolds

The release kinetics of irisin from the i/SCS/P scaffold were observed (Figure 5A). The i/SCS/P scaffolds displayed a rapid initial-burst release of protein to 28% within the first 24 hours, followed by a gradual release of up to 50% lasting another 6 days.

In vitro biological investigations

Biocompatibility of the SCS and SCS/P scaffolds

The cytotoxicities of SCS and SCS/P were evaluated through a cell counting kit-8 (CCK-8) assay (Figure 4D and E). BMSCs were seeded into standard culture medium on the culture plate with or without (control) indirect culture with the scaffold placed in the transwell. For both the SCS and SCS/P scaffolds, the BMSCs showed a stable increase of cell proliferation over time. Significant proliferation of BMSCs was found after incubation for 7 days, in contrast to the result for the corresponding group at day 1 ($P<0.05$). Similar cell proliferation compared to that of BMSCs grown on the culture plate (control) could be found. Overall, this suggested that the SCS/P scaffolds had good biocompatibility.

Effect of irisin on cell proliferation

To investigate the effect of irisin on cell proliferation, BMSCs were cultured with different concentrations of irisin for 1 day, 3 days, and 7 days, respectively. CCK-8 results (Figure 5B and C) showed that, compared with the control (no

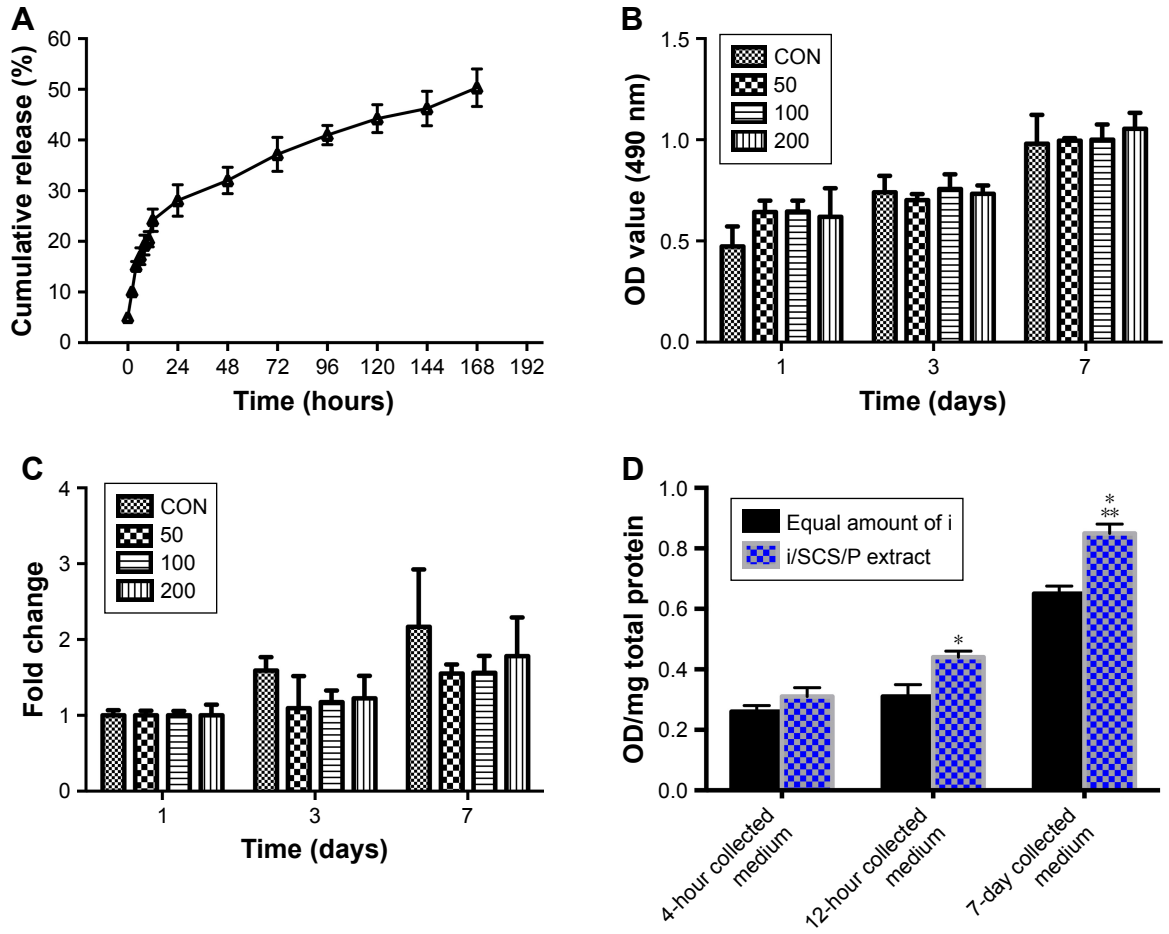

Figure 5 (*Continued*)

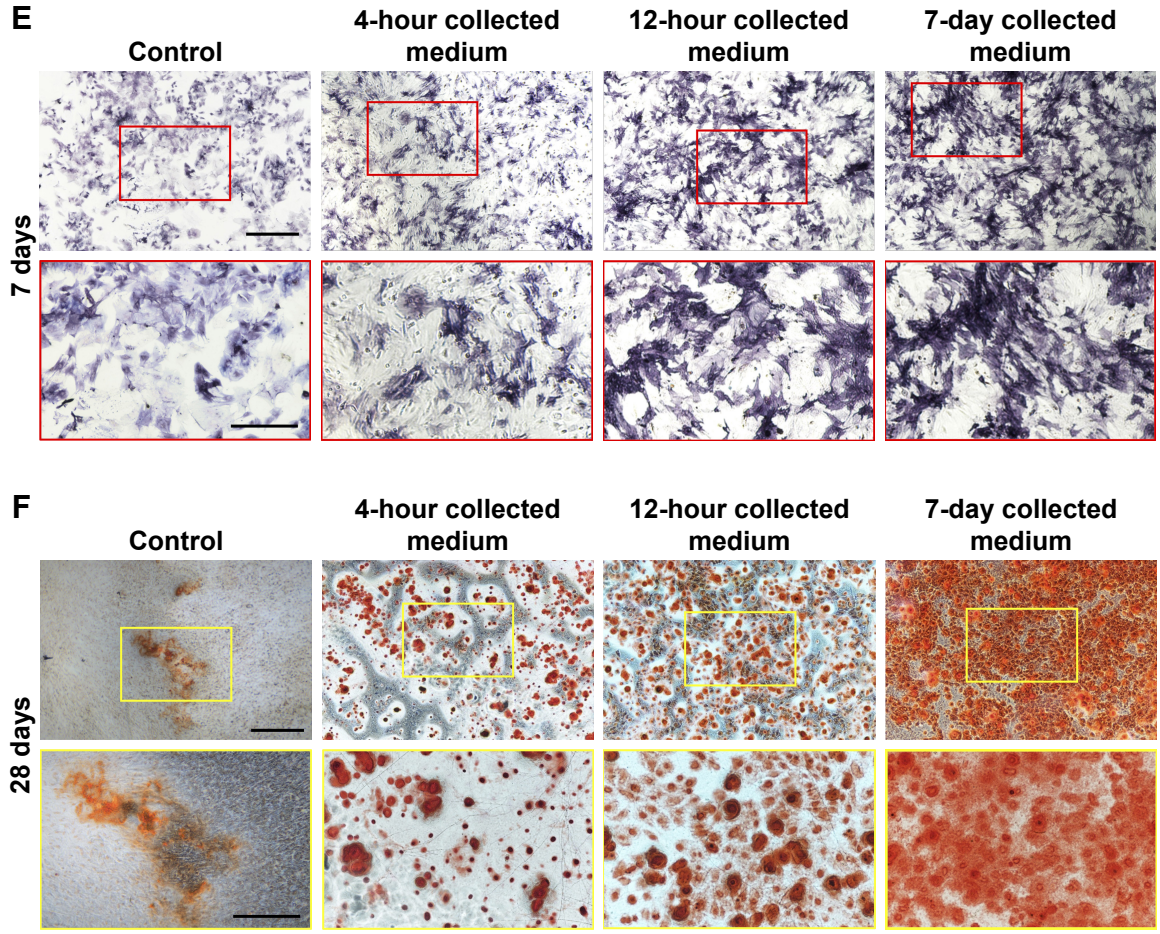

Figure 5 Bioactive release of irisin from i/SCS/P scaffold.
Notes: (**A**) Release kinetics of irisin from i/SCS/P. Effect of different concentrations of irisin on BMSCs proliferation was detected by CCK-8 and analyzed in OD values (**B**) and fold changes (**C**) compared to the corresponding control group. At each scheduled time, BMSCs cultured in standard medium without irisin were taken as control. (**D**) ALP activity assay. The i/SCS/P scaffold was immersed in culture medium for 4 hours, 12 hours, and 7 days, respectively. The extracts at different times were used to culture BMSCs for 3 days and then treated with ALP activity assay. Culture medium with a same concentration of irisin, corresponding to what was calculated in the extract, was used as positive control. *$P<0.05$, compared with the corresponding positive control group. **$P<0.05$, compared with the 4 hours and 12 hours collected medium. (**E**) ALP staining at 7 days and (**F**) ARS staining at 28 days. BMSCs were cultured with the different extracts of i/SCS/P. BMSCs cultured with the extracts of SCS/P scaffolds were used as control. Lower magnification images (scale bar: 1 mm) are shown in the upper panel. The region of interest is selected by a red or yellow box and magnified with higher magnification (scale bar: 500 μm) in the lower panel.
Abbreviations: CON, control; I, irisin; i/SCS/P, irisin-loaded silk/calcium silicate/sodium alginate/PVA; BMSCs, bone marrow stem cells; CCK-8, cell counting kit-8; ALP, alkaline phosphatase; ARS, alizarin red S; SCS/P, silk/calcium silicate/sodium alginate/PVA.

irisin treatment), no significant change in cell proliferation was found in the BMSCs treated with irisin. In other words, irisin showed no cytotoxicity toward BMSCs.

Bioactivity of the released irisin

To evaluate whether the bioactivity of irisin was attenuated after release from the i/SCS/P scaffold, the ALP activity induced by the extracts of i/SCS/P in standard culture medium respectively collected at 4 hours, 12 hours, and 7 days were investigated. Equal amounts of irisin corresponding to the different collection times were applied to BMSCs as positive controls. ALP expression is an early marker of osteogenic differentiation, while ALP activity reflects the ability of osteoblasts to synthesize type I collagen and form bone matrix.[43] As shown in Figure 5D, BMSCs incubated with irisin released from i/SCS/P showed effective upregulation of ALP activity with time. The collected 7-day extract induced significant enhancement of the ALP activity collected at 4 hours and 12 hours. Moreover, compared with the positive controls, the medium containing equal amounts of irisin corresponding to the 12-hour and 7-day collected medium showed significant differences in ALP activity. It has been speculated that loading into the SCS/P scaffold had no harmful influence on the osteogenic ability of irisin, and there was a possible synergistic effect between the SCS/P scaffold and irisin contributed by the pro-osteogenesis capacity of the SCS scaffold.[26] The in vitro osteogenic differentiation induced by the released irisin was visualized by ALP staining after

7 days (Figure 5E). Compared with the control group (extract of SCS/P), all extracts of the i/SCS/P scaffold collected at different times showed stronger positive staining, appearing dark purple, and the strongest result was found for the 7-day collected medium. This result is mainly associated with the highest concentration of irisin in the 7-day extract. Similar results could be found from the ARS staining after 28 days of culture (Figure 5F), which was used for visualization of the mineralization in vitro. These results indicated that the bioactivity of the irisin released from the i/SCS/P scaffold was not affected. Irisin may synergistically promote the osteogenic differentiation of BMSCs in vitro along with the SCS/P scaffold.

Relative gene expression of osteogenic markers

We conducted PCR analysis to examine the relative gene expression of osteogenic markers induced in vitro by i/SCS/P scaffolds (Figure 6). When BMSCs were cultured with the

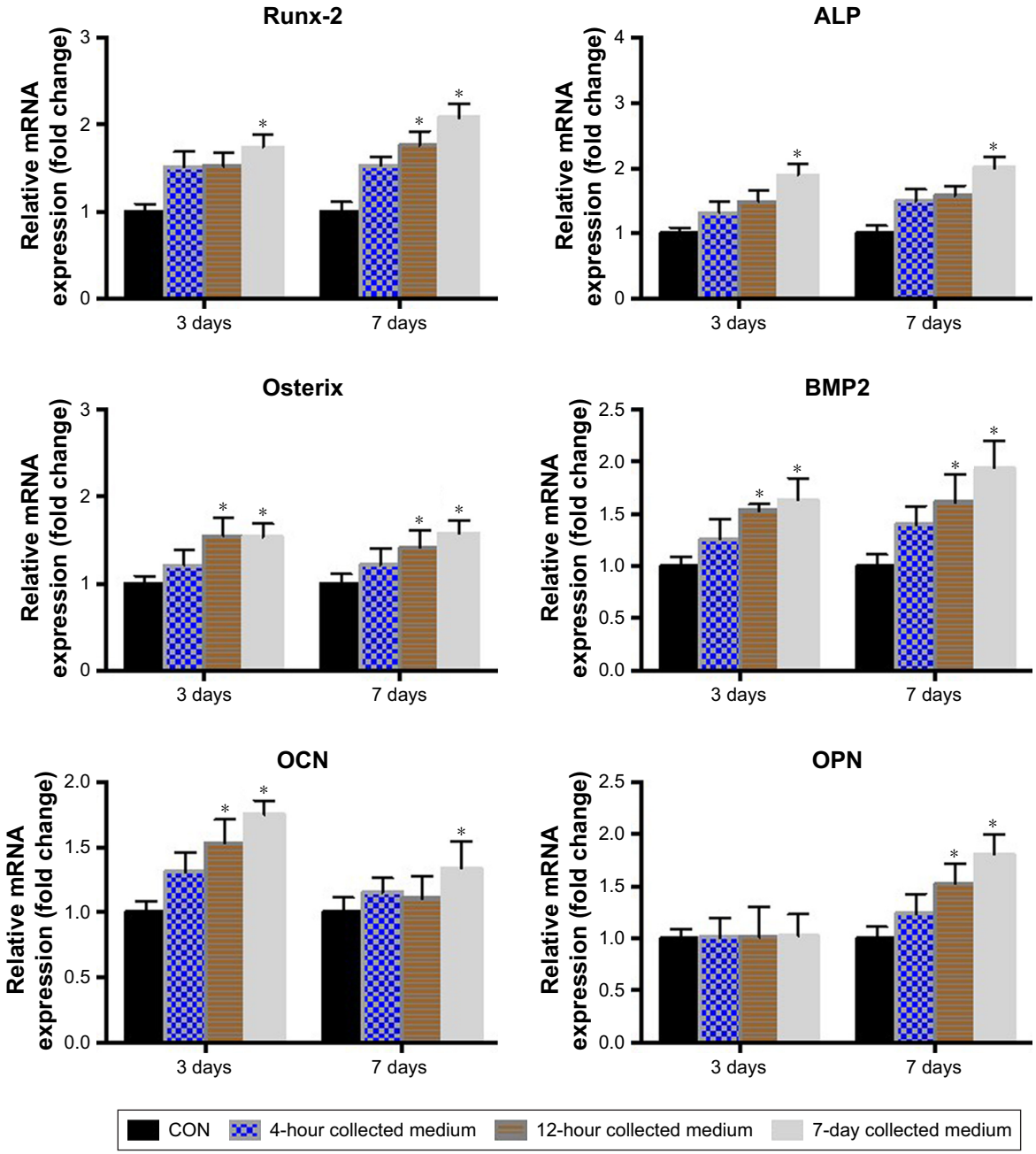

Figure 6 Relative gene expression of osteogenic markers.
Notes: BMSCs were cultured with the different extracts of i/SCS/P for 3 and 7 days, respectively. BMSCs cultured with the extracts of SCS/P scaffolds were used as control. Relative gene expressions of RUNX-2, ALP, Osterix, BMP2, OCN, and OPN were determined by PCR. *$P<0.05$, compared with the corresponding control group.
Abbreviations: BMSCs, bone marrow stem cells; i/SCS/P, irisin-loaded silk/calcium silicate/sodium alginate/PVA; SCS/P, silk/calcium silicate/sodium alginate/PVA.

7-day extract of the i/SCS/P scaffold for 7 days, the gene expression of all the osteogenic differentiation markers increased significantly compared with those from the 7-day extracts of the SCS/P scaffold (control group with no irisin released) ($P<0.05$). For the 12-hour collected medium, the relative gene expression of Osterix, BMP2, and OCN after 3 days of culture were significantly promoted compared with those of the control group ($P<0.05$), while RUNX-2, Osterix, BMP2, and OPN expressions were significantly promoted after 7 days of culture ($P<0.05$). For the 4-hour collected medium, almost no significance could be found in comparison with the control group. The PCR results showed that the i/SCS/P scaffolds help promote the gene expression of osteogenic differentiation markers of BMSCs, and the trend was similar to those observed from the ALP activity assay and staining, as well as from the ARS staining (Figure 5E and F). These findings suggested that the i/SCS/P scaffolds were capable of promoting the osteogenesis of BMSCs in vitro.

In vivo bone regeneration

μCT analysis

The morphology of the newly formed bone in the cranial defect at 8 weeks post-implantation was reconstructed by μCT (Figure 7A). The blank group, without an implanted scaffold, showed nearly no new bone formation at 8 weeks. Without irisin loading, the SCS/P scaffolds also could induce some trabecular bone formation at the defect site. The SCS/P scaffold played a key role in bone conduction, providing access and growth space for cells in the surrounding tissue and, thereby, inducing the slow formation of new bone at the defect site. According to our previous study,[26] the composition of the SCS/P scaffold could also promote osteogenesis. Much more new bone was observed in the bone defect area in the group with i/SCS/P containing 100 ng irisin, which showed that the bioactive factor, irisin, increased the healing rate of the bone defect. With a further enhanced dosage of irisin (200 ng) in the i/SCS/P scaffold, the volume of newly formed bone protruding into the bone defect was further increased, and the defect was nearly completely repaired. Moreover, quantification of the newly formed bone provided support for the results of the μCT images (Figure 7B and C). The new BV and BMD were significantly higher in the irisin-loaded groups compared to those in the blank and SCS/P scaffold groups ($P<0.05$).

Histology

Correspondingly, H&E staining images of the new bone formation induced by the above four groups are presented in Figure 8. The blank group with no implant formed fibrous tissue at the defect site at 8 weeks. There was only

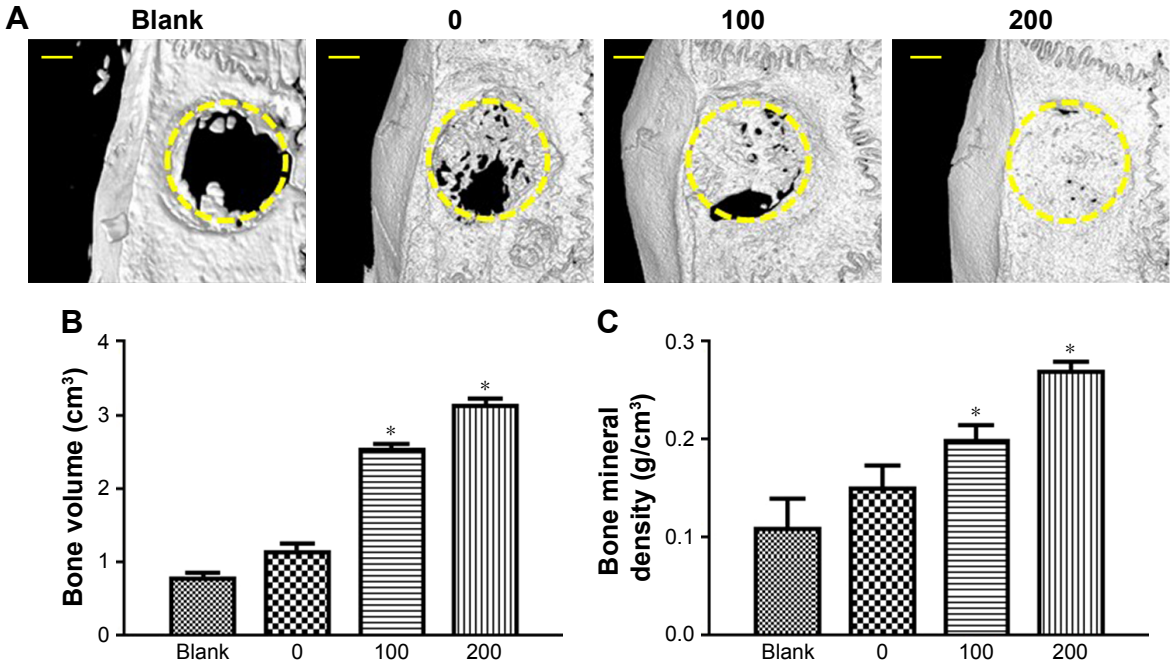

Figure 7 Evaluation of new bone formation in calvarial defects at 8 weeks post-implantation via μCT.

Notes: (**A**) Representative μCT images of calvarial defects showing mineralized bone formation after treatment with no implant (blank), SCS/P scaffold (0), i/SCS/P containing 100 ng irisin (100), and i/SCS/P containing 200 ng irisin (200), respectively. The yellow circle indicates the original defect margin. Scale bar: 1 mm. Quantitative analysis of (**B**) the volume of the regenerated BV and (**C**) BMD. *$P<0.05$, compared with blank and 0 groups.

Abbreviations: μCT, microcomputed tomography; SCS/P, silk/calcium silicate/sodium alginate/PVA; i/SCS/P, irisin-loaded silk/calcium silicate/sodium alginate/PVA; BV, bone volume; BMD, bone mineral density.

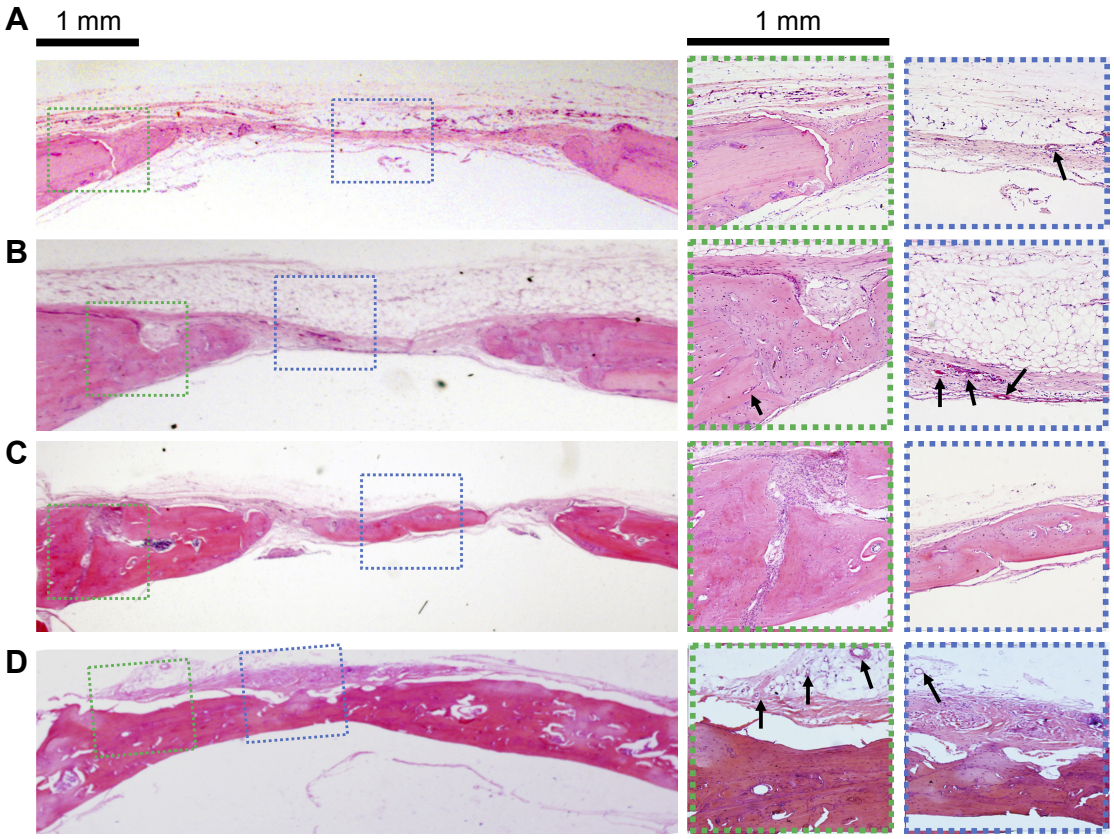

Figure 8 Histological sections stained with H&E.
Notes: Scaffolds in different groups were implanted at the calvarial defects for 8 weeks. (**A**) No implant. (**B**) SCS/P scaffold. (**C**) i/SCS/P containing 100 ng irisin. (**D**) i/SCS/P containing 200 ng irisin. The first panel images showed the whole view of the operation site. Higher magnification (×25) of the boxed area is displayed for margin of the defects (green dotted lines) and center of the defects (blue dotted lines). Black arrows represent new blood vessels and endotheliocytes.
Abbreviations: SCS/P, silk/calcium silicate/sodium alginate/PVA; i/SCS/P, irisin-loaded silk/calcium silicate/sodium alginate/PVA.

a small amount of new bone formation at the margins of the defect (Figure 8A). In the SCS/P group (Figure 8B), with the empty SCS/P scaffolds implanted, no obvious new bone but many new blood vessels could be found within the defect area, which predicted that although the SCS/P scaffold did not have enough osteoinductive capacity, it was biocompatible and provided a satisfactory porous structure for cell ingrowth and formation of a microvessel network. More newly formed bone was integrated with the native bone tissue compared with the result in the blank group. In the 100 ng irisin-containing group (Figure 8C), there was a remarkable layer of new bone formed. There was almost no material remaining but was still some unrepaired area. With the increase of irisin to 200 ng per scaffold (Figure 8D), the defect was fully bridged with a larger amount of new bone formation at 8 weeks. The boundary between the new bone and native bone could not easily be found, and plenty of vasculogenesis occurred at some sites in the bone trabecular, with the appearance of a few endotheliocytes. It has been reported that irisin could induce and promote angiogenesis through the extracellular-signal-regulated kinase signaling pathway in vitro and in vivo.[44,45] As a result, in the group with the 200 ng irisin-loaded SCS/P scaffolds, the quickest bone formation rate accompanied by the best bone quality was not only attributed to the good biocompatibility and suitable structure of the SCS/P scaffold but also to the pro-osteogenesis and pro-angiogenesis effects of irisin.

Conclusion

i/SCS/P scaffolds were developed in this study with SF, CS, and SA for irisin loading, followed by coating with PVA, which was considered to be useful for bone regeneration. The porous SCS/P scaffolds showed ~50% degradation after 28 days in PBS and a stable pH value of 7.2, which was suitable for cell growth. Meanwhile, the controlled release of irisin from the SCS/P scaffold was realized. From the in vitro experiment, we found that the released irisin from the SCS/P scaffold was maintained bioactive and capable of promoting osteogenic differentiation of BMSCs. Moreover, the i/SCS/P scaffold induced more regenerated bone with better quality after 8 weeks in vivo. Overall, the i/SCS/P system possessed

osteoinductive capability to regulate biomineralization and improve bone regeneration.

Acknowledgments

This study was supported by the National Natural Science Foundation of China (81620108006, 31500787, 81430012, 51703127, 81801006, 31600777), the National Key Research and Development Program of China (2016YFC1102900), Young Elite Scientist Sponsorship Program by CAST (2017QNRC001), and Shanghai Sailing Program (16YF1406600).

Disclosure

The authors report no conflicts of interest in this work.

References

1. Buckwalter JA, Cooper RR. Bone structure and function. *Instr Course Lect*. 1987;36:27–48.
2. Florencio-Silva R, Sasso GR, Sasso-Cerri E, Simões MJ, Cerri PS. Biology of bone tissue: structure, function, and factors that influence bone cells. *Biomed Res Int*. 2015;2015:421746.
3. Lebensohn JE. Bone structure and metabolism. *Br Med J*. 1957;37(9):469–474.
4. Müller R. Hierarchical microimaging of bone structure and function. *Nat Rev Rheumatol*. 2009;5(7):373–381.
5. Wang Q, Cao L, Liu Y, et al. Evaluation of synergistic osteogenesis between icariin and BMP2 through a micro/meso hierarchical porous delivery system. *Int J Nanomedicine*. 2017;12:7721–7735.
6. Barabaschi GD, Manoharan V, Li Q, Bertassoni LE. Engineering prevascularized scaffolds for bone regeneration. *Adv Exp Med Biol*. 2015;881:79–94.
7. Zhao P, Gu H, Mi H, Rao C, Fu J, Turng LS. Fabrication of scaffolds in tissue engineering: a review. *Front Mech Eng*. 2018;13(1):107–119.
8. Junior AL, Pinheiro CCG, Fernandes TL, Bueno DF. The use of human dental pulp stem cells for in vivo bone tissue engineering: a systematic review. *J Tissue Eng*. 2018;9(3):204173141775276.
9. Turnbull G, Clarke J, Picard F, et al. 3D bioactive composite scaffolds for bone tissue engineering. *Bioact Mater*. 2018;3(3):278–314.
10. Bose S, Tarafder S. Calcium phosphate ceramic systems in growth factor and drug delivery for bone tissue engineering: a review. *Acta Biomater*. 2012;8(4):1401–1421.
11. Porter JR, Ruckh TT, Popat KC. Bone tissue engineering: a review in bone biomimetics and drug delivery strategies. *Biotechnol Progr*. 2010;25(6):1539–1560.
12. Colaianni G, Grano M. Role of irisin on the bone-muscle functional unit. *Bonekey Rep*. 2015;4:765.
13. Dunstan D. Diabetes: exercise and T2DM-move muscles more often! *Nat Rev Endocrinol*. 2011;7(4):189–190.
14. Baxter-Jones ADG, Kontulainen SA, Faulkner RA, Bailey DA. A longitudinal study of the relationship of physical activity to bone mineral accrual from adolescence to young adulthood. *Bone*. 2008;43(6):1101–1107.
15. Cinti S. Adipocyte differentiation and transdifferentiation: plasticity of the adipose organ. *J Endocrinol Invest*. 2002;25(10):823–835.
16. Colaianni G, Cinti S, Colucci S, Grano M. Irisin and musculoskeletal health. *Ann N Y Acad Sci*. 2017;1402(1):5–9.
17. Rodríguez A, Becerril S, Ezquerro S, Méndez-Giménez L, Frühbeck G. Crosstalk between adipokines and myokines in fat browning. *Acta Physiol (Oxf)*. 2017;219(2):362–381.
18. Pardo M, Crujeiras AB, Amil M, et al. Association of irisin with fat mass, resting energy expenditure, and daily activity in conditions of extreme body mass index. *Int J Endocrinol*. 2014;2014(7):1–9.
19. Wu MV, Bikopoulos G, Hung S, Ceddia RB. Thermogenic capacity is antagonistically regulated in classical brown and white subcutaneous fat depots by high fat diet and endurance training in rats: impact on whole-body energy expenditure. *J Biol Chem*. 2014;289(49):34129–34140.
20. Colaianni G, Cuscito C, Mongelli T, et al. The myokine irisin increases cortical bone mass. *Proc Natl Acad Sci U S A*. 2015;112(39):12157–12162.
21. Si B, Gaspa G, Tabacco G. Irisin as a regulator of bone and glucose metabolism: a narrative review. *Minerva Endocrinol*. 2018;43(4):489–500.
22. Yan J, Liu HJ, Guo WC, Yang J. Low serum concentrations of irisin are associated with increased risk of hip fracture in Chinese older women. *Joint Bone Spine*. 2018;85(3):353–358.
23. McClements DJ. Encapsulation, protection, and delivery of bioactive proteins and peptides using nanoparticle and microparticle systems: a review. *Adv Colloid Interface Sci*. 2018;253:1–22.
24. Kolambkar YM, Boerckel JD, Dupont KM, et al. Spatiotemporal delivery of bone morphogenetic protein enhances functional repair of segmental bone defects. *Bone*. 2011;49(3):485–492.
25. Gehrke SH, Uhden LH, McBride JF. Enhanced loading and activity retention of bioactive proteins in hydrogel delivery systems. *J Control Release*. 1998;55(1):21–33.
26. Zheng A, Cao L, Liu Y, et al. Biocompatible silk/calcium silicate/sodium alginate composite scaffolds for bone tissue engineering. *Carbohydr Polym*. 2018;199:244–255.
27. Brenmoehl J, Albrecht E, Komolka K, et al. Irisin is elevated in skeletal muscle and serum of mice immediately after acute exercise. *Int J Biol Sci*. 2014;10(3):338–349.
28. Dorniani D, Au K, Hussein-Al-Ali SH. In vitro sustained release study of gallic acid coated with magnetite-PEG and magnetite-PVA for drug delivery system. *ScientificWorldJournal*. 2014;2014:416354.
29. Lin B, Zheng CZ, Zhao MH, Wu PQ, Gu WX, Lu QM. Preparation and characterization of boron controlled-release film as a potential coating material. *Mater Sci Forum*. 2016;852:1060–1065.
30. Muschert S, Siepmann F, Leclercq B, Carlin B, Siepmann J. Drug release mechanisms from ethylcellulose: PVA-PEG graft copolymer-coated pellets. *Eur J Pharm Biopharm*. 2009;72(1):130–137.
31. Takeuchi H, Kojima H, Yamamoto H, Kawashima Y. Polymer coating of liposomes with a modified polyvinyl alcohol and their systemic circulation and RES uptake in rats. *J Control Release*. 2000;68(2):195–205.
32. Brown J, Lu CL, Coburn J, Kaplan DL. Impact of silk biomaterial structure on proteolysis. *Acta Biomater*. 2015;11:212–221.
33. Kokubo T, Kushitani H, Sakka S, Kitsugi T, Yamamuro T. Solutions able to reproduce in vivo surface-structure changes in bioactive glass-ceramic A-W3. *J Biomed Mater Res*. 1990;24(6):721–734.
34. Jiang X, Zhao J, Wang S, et al. Mandibular repair in rats with premineralized silk scaffolds and BMP-2-modified bMSCs. *Biomaterials*. 2009;30(27):4522–4532.
35. Xu L, Lv K, Zhang W, Zhang X, Jiang X, Zhang F. The healing of critical-size calvarial bone defects in rat with rhPDGF-BB, BMSCs, and β-TCP scaffolds. *J Mater Sci Mater Med*. 2012;23(4):1073–1084.
36. Lin S, Zhang Q, Cao Z, et al. Constitutive nuclear expression of dentin matrix protein 1 fails to rescue the *Dmp1*-null phenotype. *J Biol Chem*. 2014;289(31):21533–21543.
37. Karageorgiou V, Kaplan D. Porosity of 3D biomaterial scaffolds and osteogenesis. *Biomaterials*. 2005;26(27):5474–5491.
38. Peng Y, Liu QJ, He T, Ye K, Yao X, Ding J. Degradation rate affords a dynamic cue to regulate stem cells beyond varied matrix stiffness. *Biomaterials*. 2018;178:467–480.
39. Disthabanchong S, Radinahamed P, Stitchantrakul W, Hongeng S, Rajatanavin R. Chronic metabolic acidosis alters osteoblast differentiation from human mesenchymal stem cells. *Kidney Int*. 2007;71(3):201–209.
40. Rice RW. Comparison of stress concentration versus minimum solid area based mechanical property-porosity relations. *J Mater Sci*. 1993;28(8):2187–2190.
41. Lin X, Shi Y, Cao Y, Liu W. Recent progress in stem cell differentiation directed by material and mechanical cues. *Biomed Mater*. 2016;11(1):014109.

42. Hudson JE, Frith JE, Donose BC, et al. A synthetic elastomer based on acrylated polypropylene glycol triol with tunable modulus for tissue engineering applications. *Biomaterials*. 2010;31(31):7937–7947.
43. Basdra EK, Komposch G. Osteoblast-like properties of human periodontal ligament cells: an in vitro analysis. *Eur J Orthod*. 1997;19(6):615–621.
44. Song H, Wu F, Zhang Y, et al. Irisin promotes human umbilical vein endothelial cell proliferation through the ERK signaling pathway and partly suppresses high glucose-induced apoptosis. *PLoS One*. 2014;9(10):e110273.
45. Wu F, Song H, Zhang Y, et al. Irisin induces angiogenesis in human umbilical vein endothelial cells in vitro and in zebrafish embryos in vivo via activation of the ERK signaling pathway. *PLoS One*. 2015;10(8):e0134662.

Supplementary material

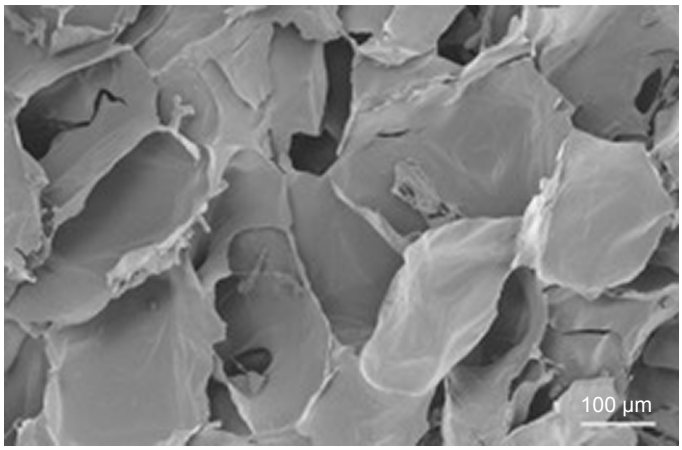

Figure S1 SEM image of cross section of the SCS/P scaffold.
Abbreviations: SEM, scanning electron microscopy; SCS/P, silk/calcium silicate/sodium alginate/PVA.